

First Results of ECE Measurements at the GDT Mirror Trap

A. L. Solomakhin^{1,2, a)}, P. A. Bagryansky¹, E. D. Gospodchikov^{1,3},
L. V. Lubyako^{1,3}, A. G. Shalashov^{1,3} and D. V. Yakovlev^{1,2}

¹*Budker Institute of Nuclear Physics, Siberian Branch of Russian Academy of Sciences, Novosibirsk, Russia*

²*Novosibirsk State University, Novosibirsk, Russia*

³*Institute of Applied Physics of Russian Academy of Sciences, Nizhny Novgorod, Russia*

^{a)}Corresponding author: A.L.Solomakhin@inp.nsk.su

Abstract. The paper summarizes the results of experiments on electron cyclotron emission (ECE) measurements recently performed at the GDT magnetic mirror device. The new ECE diagnostics is installed to facilitate the successful ECRH experiment and operates in the vicinity of the ECRH frequency 54.5 GHz. The particulars of plasma emission at the fundamental electron cyclotron harmonic are studied experimentally in a broad range of discharge scenarios.

INTRODUCTION

The gas dynamic trap (GDT) in the Budker Institute is an axially symmetric open magnetic trap with a large mirror ratio (up to $R = 35$) [1]. The trap is the prototype of a powerful source of fusion neutrons, with a number of perspective applications, including fusion material testing, a hybrid fusion-fission reactor and nuclear waste processing [2]. At the GDT, neutrons are born as a result of thermonuclear reactions in collisions between hot ions driven by high-power neutral (atomic deuterium) beam injection (NBI). Lifetime of hot deuterons in stationary conditions at the GDT is proportional to the electron temperature to power $3/2$, so the increase of the temperature of bulk electrons is a key approach to increase the neutron flux [3-6]. This purpose is served by additional electron cyclotron resonance plasma heating (ECRH), based on the capture and absorption of high-power microwave beams generated by two 400 kW / 54.5 GHz gyrotrons of "Buran-A" type [6]. With high-power transmission line made of oversized corrugated waveguide, the radiation is delivered to two quasi-optical launching ports located symmetrically at both ends of the trap near the magnetic mirrors. The wave beams are launched into the plasma from the high magnetic field side at an optimal angle about 36° to the trap axis.

ECRH system is operating at the fundamental harmonic of the extraordinary (X) mode. The plasma conditions near the ECR are arranged such that the wave beam is trapped by the plasma waveguide and delivered to the ECR, where it is absorbed completely [4]. This completely new ECRH scenario depends neatly on the magnetic configuration and the plasma inhomogeneity. Although successful ECRH experiment at the GDT evidences in favor of reliability of such heating mechanism [5, 6], the new electron cyclotron emission (ECE) diagnostics has been recently installed to facilitate understanding the EC wave physics at the GDT conditions. The original idea was to exploit the reciprocity principle and Kirchhoff's law that link the absorption and the spontaneous emission of the plasma in thermal equilibrium [7]. So, the conditions favorable for ECR plasma heating should manifest themselves in thermal EC emission. According to this idea, the ECE diagnostics operates in the vicinity of the ECRH frequency 54.5 GHz in the geometry reversed with respect to the ECRH. In practice, we connect the ECE receiver to the high-power transmission line instead of one of the gyrotrons. As a result, the ECE measurements use all advantages provided by the ECRH transmission system, such as good coupling efficiency, low transit losses and good polarization control with a dedicated universal polarizer mounted in the ECRH line.

HARDWARE AND EXPERIMENTAL CONDITIONS

ECE detection is based on specially designed heterodyne radiometer with block scheme shown in Fig. 1. The receiver is operating in 54–59.5 GHz frequency range with HF bandwidth 100 MHz, VF bandwidth 35 kHz, noise temperature about 0.2 eV, and fluctuation sensitivity $3 \cdot 10^{-3}$ eV. At the input, the received RF signal passes through the electronic p-i-n attenuator, which can operate either in controlled attenuation range of 0-40 dB, or in the external lock mode with maximum attenuation of 50 dB. The last mode is used to protect sensitive radiometer circuits from the powerful gyrotron radiation. As such protection is very critical, the dedicated notch filter tuned to black out the gyrotron frequency (54.5 GHz) and the high-pass filter with the cutoff frequency near 55 GHz have been installed and used during the experiments. A single-balanced mixer is used to detect the received RF signal. The local oscillator is based on Gunn diode with tunable frequency. It is isolated from the rest of the tract by a ferrite valve. The intermediate frequency signal is amplified by 60 dB by a broadband IF amplifier. The frequency band of the radiometer is determined by a band pass filter 1.63 ± 0.05 GHz. The signal is detected by a square-law detector and comes to two-stage video amplifier with 25+10 dB gain and 0-35 kHz band. Variable attenuator 0-25 dB is set between these components. The signal is recorded with an external ADC. The radiometer provides a second output, which is equipped with an integrating chain with $\tau = 1$ s and used in calibrating of the radiometer with a "black body" microwave load with a known radiation temperature. In this way, the ECE system is calibrated for absolute measurements of the radiation temperature of the detected emission.

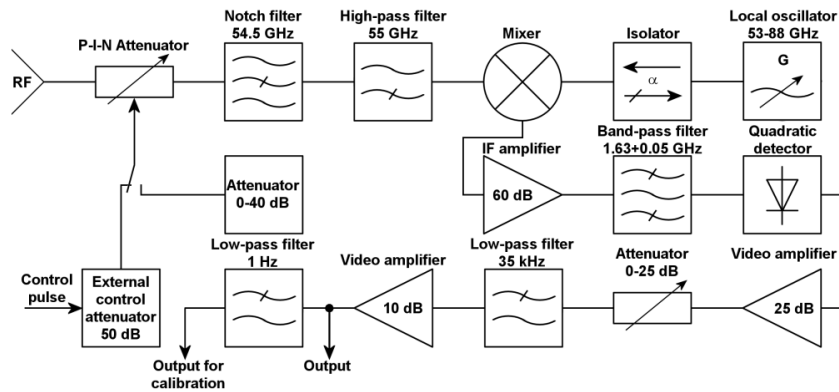


FIGURE 1. Block diagram of the radiometer.

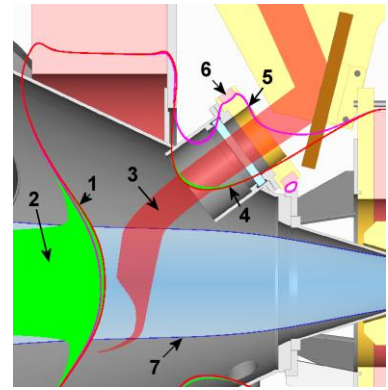


FIGURE 2. ECRH zone and ECE.

As already mentioned, in the reported ECE experiments we use the exciting ECRH launching port. Figure 2 shows the received emission pattern and the plasma configuration near the receiving antenna. An important feature of X wave propagation near the fundamental cyclotron harmonic is inaccessibility of the ECR layer (1 in Fig. 2) from the low (relative to the resonance) magnetic field side due to presence of the evanescent region (2 in Fig. 2) just outside the ECR in which the X mode cannot propagate. Exactly for this reason, the waves (3 in Fig. 2) are launched from the high field side in the present ECRH scheme. However, since the gyrotron is located far away from the GDT in the low field, its radiation inevitably meets an auxiliary ECR surface from the low field side. In GDT conditions, this surface (4 in Fig. 2) is located in the launching port inside the vacuum chamber, where some residual plasma may result in radiation reflection. This so-called "parasitic" ECR plays an important role in optimizing of the ECRH conditions at the GDT, as well as in the interpretation of the ECE data. In particular, the "parasitic" ECR can be shifted (5 in Fig. 2) far from the plasma boundary to the wall of the vacuum chamber by increasing the current through the nearest axial coil of the GDT magnetic system, or by applying the small correction coil (6 in Fig. 2) which is fixed near the microwave vacuum. Highlighted plasma volume (7 in Fig. 2) indeed corresponds to the dense plasma boundary ($n_e > 2 \times 10^{12} \text{ cm}^{-3}$), although less dense residual plasma outside this volume may still affect the wave propagation.

Another peculiar feature of the reported ECE experiments is related to variation in time of the confining magnetic field during a discharge. This is important for the measurements at plasma decay stage when the variation of the magnetic field is essential. Indeed, variation of the cyclotron frequency ω_b in the cyclotron resonance condition, $\omega_b(t) = \gamma(\omega - k_{\parallel}v_{\parallel})$ is equivalent to measuring of ECE spectrum even though the receiver is operating

with a fixed radiation frequency ω (here k_{\parallel} and v_{\parallel} are projections of a wave vector and an electron velocity on the magnetic field direction, γ is a relativistic factor for the emitting electron). This information provides a key to distribution function of the emitting electrons over velocities or energies.

In experiments we detected two types of ECE signal. In purely NBI discharges and at early stages of discharges with additional ECRH, the observed ECE was interpreted as thermal emission of bulk electrons with Maxwellian distribution. Contrary, at late stages of ECRH discharges, this thermal ECE was totally suppressed by a strong signal which may be attributed to cyclotron emission of suprathermal electrons generated during ECRH.

CYCLOTRON EMISSION OF THERMAL ELECTRONS

Measured thermal ECE signals have validated the existing physical conceptions about the EC resonance heating of plasma in the machine, in particular the significance of the auxiliary ECR surface in the launching port that affects the wave propagation in core plasma. A typical example is shown in Fig. 3, where we plot the time-traces for the measured X mode ECE intensity in terms of the effective radiation temperature (T_{rad}) [7]. Measurements were carried out at the frequency range 55.2 ± 0.05 GHz. The figure shows two ECE signals measured with ($I_{\text{cc}} = 1$ kA) and without ($I_{\text{cc}} = 0$ kA) the correction coil for the “parasitic” resonance. Also the figure shows dependence of the magnetic field near the microwave window on time as measured by a dedicated diagnostic coil. The magnetic field is shown in units of the electron cyclotron frequency $eB/2\pi mc$. The figure indicates the reference value of the electron temperature T_{is} measured with Thomson scattering laser system and the time of this measurement. One can clearly see that, when the magnetic field exceeds a resonant value corresponding to the receiving frequency (55.2 GHz), the difference between ECE signals increases dramatically. Switching-on of the correction coil results in further increase of the ECE level up to factor of two. Since the correction coil does not affect the main ECR, it can be concluded that the “parasitic” ECR should significantly affect the passage of radiation though the launching port (both for ECE and ECRH).

Note that the electron temperature measured by Thomson scattering is by about an order of magnitude greater than the effective temperature of thermal ECE, e.g. $T_{\text{is}} = 180$ eV versus $T_{\text{rad}} = 22$ eV for example in Fig. 3. It indicates potentially poor efficiency of the ECRH in studied configuration, at least at the initial stage. At the same time, ECE measurements shows that shift of the “parasitic” resonance from the vacuum chamber by the correction coil may substantially improve the efficiency ECRH.

Comparison of the ECE in cross-polarizations (X and O modes) are in reasonable agreement with theoretical predictions (ray-tracing) for the moderately warm Maxwellian electrons with temperatures about 100-200 eV.

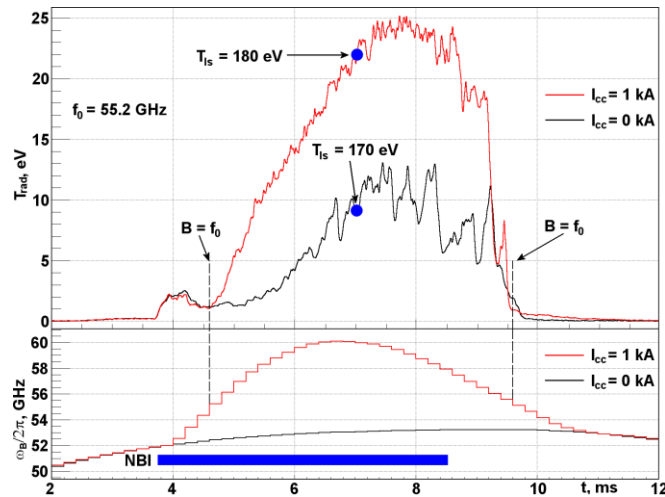


FIGURE 3. ECE radiation temperature and magnetic field near the microwave launching port in the GDT discharge without ECRH with (red lines) and without (black lines) the correction coil for the “parasitic” resonance.

CYCLOTRON EMISSION OF SUPRATHERMAL ELECTRONS

A strong increase of ECE level was observed in the experiments with ECRH on. What was more intriguing is that this signal was also repeatedly observed after the total decay of the main plasma and in both (X and O) polarizations. These features allow interpreting these signals as ECE from population of fast electrons produced by ECRH. With energies of 100 keV and higher, these electrons are confined adiabatically. They interact weakly with the bulk plasma, so they can live in the trap much longer after the collapse of the main plasma. A typical example is presented in Fig. 4 which shows a number of ECE traces for various frequencies and polarizations, the magnetic field near the axis (as measured by a special coil) and the linear plasma density. Each ECE signal is measured in a separate discharge of the series of identical shots. Note that the radiometer input was blocked during the gyrotron operation, so only ECE data just before and after the ECRH phase. One can see that the X mode ECE level essentially increases during the ECRH, then it decreases as the plasma decays, but then it sharply increases again when the bulk plasma is already completely decayed. The O mode signal does not reduce to zero at the plasma decay, it monotonically decreases still characterizing a fairly high level at late stages with no bulk plasma. Also Fig. 4 shows the signal of the standard neutron detector, which potentially measures the X-ray during the reported experiment. Indeed, the neutron flux stops after approximately 1 ms after the end of the NBI, thus the rest signal may be attributed to the X-ray radiation produced by fast electrons with energies at least 100 keV (as required for the transmission of X-rays through 5 mm thick stainless steel wall of the vacuum chamber).

As mentioned above, the time traces of ECE intensity with varying external magnetic fields may be used for recovering the electron distribution function. For example shown in Fig. 4, the frequency shift is $(\omega - \omega_p)/\omega \approx 0.08 - 0.11$ in the interval between 15 and 25 ms. This corresponds to the Doppler shift $\Delta\omega = k_{\parallel}v_{\parallel}$ by electrons with the longitudinal energy about 5 keV or the relativistic shift $\Delta\omega = (\gamma - 1)\omega$ by electrons with total energy about 100 keV. The latter agrees with theoretical limit of maximum energy due the resonance escape outside the microwave beam for the relativistic electrons. More accurate analysis confirms that the energy spectrum of suprathermal electrons lays in the range 5 – 100 keV what is in good agreement with our study of the electron kinetics during the ECR breakdown [8, 9]. The "gap" for the X mode emission is most likely related to a topological bifurcation of the ECR surface.



FIGURE 4. ECE radiation temperature, magnetic field at the GDT axis, X-ray signal and linear plasma density in the discharge with combined NBI and ECRH plasma heating.

CONCLUSION

The new ECE diagnostics has been installed to facilitate the ECRH experiment. The particulars of plasma cyclotron emission in the vicinity of the ECRH frequency were studied experimentally in a broad range of discharge scenarios in the GDT. Measured thermal spectra have validated the existing physical conceptions about the microwave plasma heating in the machine, in particular the significance of the auxiliary ECR surface in the launching port that affects the wave propagation towards the core plasma. Efficiency of the dedicated non-planar magnetic coil for the suppression of the auxiliary resonance has been validated with the thermal ECE measurements. Measured non-thermal ECE spectra have unambiguously confirmed the existence of suprathermal electrons in GDT for the first time. As it turned out, these electrons are generated by the intense microwave field during the ECR heating of the main plasma. Time dependence of ECE level corresponding to variation of confining magnetic field allowed reconstructing distribution function of suprathermal electron and estimating their population.

ACKNOWLEDGEMENTS

The research was supported by the Russian Science Foundation (pr. 14-12-01007).

REFERENCES

- [1] A. A. Ivanov and V. V. Prikhodko, *Plasma Phys. Control. Fusion* **55**, 063001 (2013).
- [2] A. V. Anikeev, P. A. Bagryansky, A. D. Beklemishev, A. A. Ivanov, E. Yu. Kolesnikov, M. S. Korzhavina, O. A. Korobeinikova, A. A. Lizunov, V. V. Maximov, S. V. Murakhtin, E. I. Pinzhenin, V. V. Prikhodko, E. I. Soldatkina, A. L. Solomakhin, Yu. A. Tsidulko, D. V. Yakovlev and D. V. Yurov, *Materials* **8**, 8452 (2015).
- [3] A. V. Anikeev, P. A. Bagryansky, A. A. Ivanov, A. N. Karpushov, S. A. Korepanov, V. V. Maximov, S. V. Murakhtin, A. Yu. Smirnov, K. Noack, and G. Otto, *Nucl. Fusion* **40**, 753 (2000).
- [4] A. G. Shalashov, E. D. Gospodchikov, O. B. Smolyakova, P. A. Bagryansky, V. I. Malygin and M. Thumm, *Phys. Plasmas* **19**, 052503 (2012).
- [5] P. A. Bagryansky, A. G. Shalashov, E. D. Gospodchikov, A. A. Lizunov, V. V. Maximov, V. V. Prikhodko, E. I. Soldatkina, A. L. Solomakhin and D. V. Yakovlev, *Phys. Rev. Lett* **114**, 205001 (2015).
- [6] P. A. Bagryansky, A. V. Anikeev, G. G. Denisov, E. D. Gospodchikov, A. A. Ivanov, A. A. Lizunov, Yu. V. Kovalenko, V. I. Malygin, V. V. Maximov, O. A. Korobeinikova, S. V. Murakhtin, E. I. Pinzhenin, V. V. Prikhodko, V. Ya. Savkin, A. G. Shalashov, O. B. Smolyakova, E. I. Soldatkina, A. L. Solomakhin, D. V. Yakovlev and K. V. Zaytsev, *Nucl. Fusion* **55**, 053009 (2015).
- [7] G. Bekefi, *Radiation Processes in Plasmas* (Wiley and Sons, New York, 1966).
- [8] A. G. Shalashov, D. V. Yakovlev, P. A. Bagryansky et al., Theory of Electron Cyclotron Resonance Startup in the Gas Dynamic Trap, *AIP Conf. Proc.* (these proceedings)
- [9] D. V. Yakovlev, A. G. Shalashov, E. D. Gospodchikov et al., Electron-cyclotron plasma startup in the GDT experiment, *ArXiv:1607.01051* [physics.plasm-ph] (2016)